Atmos. Chem. Phys. Discuss., 13, 27937–27969, 2013
www.atmos-chem-phys-discuss.net/13/27937/2013/
doi:10.5194/acpd-13-27937-2013
© Author(s) 2013. CC Attribution 3.0 License.

Atmospheric Chemistry and Physics Discussions

This discussion paper is/has been under review for the journal Atmospheric Chemistry and Physics (ACP). Please refer to the corresponding final paper in ACP if available.

Effects of aerosols on precipitation in north-eastern North America

R. Mashayekhi and J. J. Sloan

Department of Earth and Environmental Sciences, University of Waterloo, Waterloo ON N2L 3G1, Canada

Received: 7 August 2013 – Accepted: 13 October 2013 – Published: 29 October 2013

Correspondence to: J. J. Sloan (sloanj@uwaterloo.ca)

Published by Copernicus Publications on behalf of the European Geosciences Union.

Abstract

The changes in precipitation over north-eastern North America caused by chemistry – and particularly anthropogenic aerosols – are investigated using the Chemistry version of the Weather Research and Forecasting (WRF/Chem v3.4) model. The simulations were carried out for a five-month period from April to August 2009. The model results show that non-negligible changes in both convective and cloud-resolved (non-convective) precipitation are caused by chemistry and/or aerosols over most parts of the domain. The changes can be attributed to both radiative and microphysical interactions with the meteorology. A chemistry-induced change of approximately −15 % is found in the five-month mean daily convective precipitation over areas with high convective rain; most of this can be traced to radiative effects. Although, total non-convective rain is less than total convective rain in the domain, chemistry-induced effects on the former are more pronounced than those on the latter. A chemistry-induced increase of about +30 % is evident in the five-month mean daily non-convective precipitation over the heavily urbanized parts of the Atlantic coast. The effects of aerosols on cloud microphysics and precipitation were examined for two particle size ranges: 0.039–0.1 µm and 1–2.5 µm. Strongly positive spatial correlation between cloud droplet number and non-convective rain are found for activated (cloud-borne) aerosols in both size ranges. Non-activated (interstitial) aerosols have a positive correlation with cloud droplet number and non-convective rain when they are small and an inverse correlation for larger particles.

1 Introduction

The modification of climate by anthropogenic influences is the subject of intense public debate and extensive scientific research. Most of this interest is focussed on the global climate, but regional effects are in some ways more important, because they occur on a shorter timescale and can be quite intense. The so-called “urban heat is-

ACPD
13, 27937–27969, 2013

land" effect is an example of this. It has been shown that thermal effects of megacities reach considerably beyond their borders (Wu et al., 2008) and also that precipitation increases occur downwind of the cities (Auvray and Bey, 2005; Tuccella et al., 2012). These results are relevant to predictions of the consequences of future urban growth in locations that do not, at present, have extremely high population densities. For example, the Toronto–Hamilton area, which had a 2011 census population of 6.5 M, is expected to grow by more than 30 % to 8.6 M in less than three decades (Xue et al., 2001). Similar, or more rapid, growth will occur in the cities of the north-eastern United States during the same period. In this and later publications, we intend to explore the possible effects of such increases in population density on the regional climate of north eastern North America, with a focus on precipitation in southern Canada.

Although not the only anthropogenic influence on precipitation, aerosols are known to be among the most important. The precise mechanisms for these influences are complicated, but numerous observational and modeling studies have shown that precipitation is significantly influenced by atmospheric aerosols (Ackerman et al., 2000; Lohmann and Feichter, 2005; Haywood and Boucher, 2000; Ramanathan et al., 2001; Rosenfeld et al., 2006; Penner et al., 2004; Koren et al., 2005). Aerosol particles can affect cloud properties through a combination of radiative and microphysical effects (Rosenfeld et al., 2008). They can reduce convection by cooling the surface via attenuation of solar radiation (Ramanathan et al., 2001) and heat the upper atmosphere by absorption of infrared radiation (Haywood et al., 1999; Ramanathan et al., 2001). These particular effects combine to stabilize the atmosphere (Taubman et al., 2004) and reduce the generation of convective clouds (Koren et al., 2005).

In addition to radiative effects, the aerosols also affect cloud microphysics by acting as cloud condensation nuclei (CCN) (Cotton and Pielke Sr, 2007). Increasing the number of CCN creates more droplets of smaller size and increases the cloud albedo (Twomey, 1977). This can slow the process of coalescence into raindrops, suppressing the precipitation and prolonging the cloud lifetime (Haywood and Boucher, 2000; Albrecht, 1989). Based on the above description, both radiative and microphysical ef-

ACPD
13, 27937–27969, 2013

fects can cause reductions in precipitation. Our understanding of aerosol effects on precipitation, however, is still qualitative (IPCC, 2007). Some recent studies have reported an enhancement in precipitation due to aerosol effects (Rosenfeld et al., 2002; Rudich et al., 2002; Givati and Rosenfeld, 2004; Lohmann and Hoose, 2009; Khain et al., 2004; Bell et al., 2008), while others found aerosol-induced suppression (Rosenfeld and Givati, 2006; Borys et al., 2003; Andreae et al., 2004; Rosenfeld, 2000).

The response of cloud properties and precipitation to aerosols depends on many factors, including cloud types, relative humidity, atmospheric stability and aerosol characteristics such as hygroscopicity and index of refraction (Williams et al., 2002; Tao et al., 2007; Khain et al., 2005; Lynn et al., 2007). Consequently, a realistic understanding of the effects of aerosols on precipitation requires the use of models in which aerosols, meteorology, radiation and cloud microphysics couple in a fully interactive way. The Weather Research Forecasting with Chemistry (WRF/Chem) model (Grell et al., 2005) provides such interactive coupling. WRF/Chem has been used successfully to simulate aerosol-cloud interactions in a variety of situations in North America (McKeen et al., 2007; Zhang et al., 2010b; Grell et al., 2005; Chuang et al., 2011). Much of the previous work found significant changes in precipitation due to the inclusion of aerosol feedback (Rosenfeld et al., 2007; Lynn et al., 2007; Zhang et al., 2010a, b). The accuracy of the model predictions, however, depends on many factors, such as horizontal resolution, PBL turbulence parameterization and the quality of the emission inventory (McKeen et al., 2007). For this reason, the models must be carefully configured for the regions of application and their accuracy must be verified by comparison with measurements. In this study, we have used both WRF and WRF/Chem (version 3.4) to explore the effect of chemistry on the amount and distribution of precipitation over north-eastern North America. The overall effects of chemistry can be deduced from a comparison of the results obtained from WRF with those from WRF/Chem, using identical meteorological parameterizations. An understanding of the causes for the observed differences, however, requires a more detailed analysis of the results using statistical and correlative methods.

ACPD
13, 27937–27969, 2013

We created temporally and spatially distributed emission fluxes for this work using the SMOKE emission-processing model with US and Canadian emission inventories. Much of this work involved the creation of surrogate files, which not only provide reasonably accurate emission rates, but also have the advantage of flexibility for scenario studies. We will exploit this flexibility in later publications, but before reporting scenario results, we must understand how WRF/Chem predicts the influences of chemistry – and in particular aerosols – on precipitation. To do this, we will assess the accuracy with which the model can predict changes in precipitation and examine the important mechanisms involved. The latter include microphysical effects on non-convective precipitation and also thermal effects caused by cloud nucleation, which affect convective precipitation. Aerosol size has a very important influence in both mechanisms.

2 Model configuration

Section 2.1 briefly describes the model configuration options we used in this study. The emission processing is described in Sect. 2.2.

2.1 WRF/Chem model description

WRF/Chem is an online-coupled meteorology-chemistry-aerosol model being developed in a collaboration involving several agencies (NCAR, NOAA/NCEP, NOAA, ESRL and PNNL). Version 3.4 of WRF/Chem was used for this study. A detailed description of this version of the model can be found in (Grell et al., 2005; Fast et al., 2006).

WRF/Chem v3.4 has several choices for gas-phase chemical mechanisms and aerosol modules. The gas-phase chemistry in this study is based on the Carbon Bond Mechanism version Z (CBM-Z); (Zaveri and Peters, 1999), which uses 67 prognostic species and 164 reactions in a lumped structure approach. The aerosol module used in this work is the Model for Simulating Aerosol Interactions and Chemistry (MOSAIC) aerosol scheme (Zaveri et al., 2008). The aerosol size distribution was defined using

ACPD
13, 27937–27969, 2013

a sectional approach with four size-bins: 0.039–0.10 µm, 0.10–1.0 µm, 1.0–2.5 µm, and 2.5–10 µm. The major aerosol compounds including sulfate, methanesulfonate, nitrate, chloride, carbonate, ammonium, sodium, calcium, black carbon, primary organic mass, liquid water and certain other inorganic species are all included. The MOSAIC simulation calculates particle evolution via the major aerosol processes, including binary nucleation, coagulation, condensation and scavenging by cloud droplets, as well as wet and dry deposition. It also includes inorganic aerosol thermodynamic equilibrium and PM formation via aqueous-phase chemistry. In the latter, aerosol activation and resuspension are based on the approach described by (Chapman et al., 2009), using the droplet-activation parameterization of (Abdul-Razzak and Ghan, 2002), in which the aerosol activation is based on maximum supersaturation as calculated from explicitly resolved updraft velocities and aerosol properties. More detailed information about the treatment of chemistry-aerosol interactions and WRF/Chem cloud microphysics can be found in (Fast et al., 2006; Gustafson et al., 2007; Chapman et al., 2009).

Table 1 lists the configuration options used for WRF/Chem. Two sets of simulations (with and without chemistry) were carried out to assess the effects of chemistry on precipitation. The meteorological configuration was identical for both, but the chemistry options were all turned off for the meteorology-only simulation. The model domain covers the north-eastern part of North America with a $12 \times 12\,km^2$ horizontal grid; it includes 31 vertical levels extending up to approximately 16 km above mean sea level. The initial and lateral boundary conditions for meteorological parameters were obtained from the three-hourly North American Regional Reanalysis (NARR) dataset.

The initial and boundary conditions for trace gases and particulate species were taken from the MOZART-4 global model output at 3 h time intervals (Emmons et al., 2010). The model simulations were re-initialized every 3.5 days and the first 12 h of each run were discarded, allowing a 12 h spin-up period for the meteorology. The chemistry initialization was obtained from the previous run (i.e. the output from the previous simulation was used as input for the next one).

ACPD
13, 27937–27969, 2013

2.2 Emission processing

Biogenic and anthropogenic emission from various sources is considered separately in this study. Anthropogenic emissions for gases and aerosol particles were pre-processed using the Sparse Matrix Operator Kernel Emissions (SMOKE) modeling system, version 2.7, which is developed and maintained by the United States Environmental Protection Agency (US EPA) and the Carolina Environmental Program (CEP) of the University of North Carolina (Houyoux and Vukovich, 1999) (UNC, 2005). SMOKE is, inter alia, an emission processing system designed to convert raw emission inventory data to gridded, speciated, hourly emission rates suitable for input to AQMs. The following sections give more details about anthropogenic and biogenic emission fluxes used in this study.

2.2.1 Anthropogenic emissions

For these, we used the total annual, province-based Canadian emission inventory for the year 2006 provided by Environment Canada and the corresponding county-based US inventories for 2008 from the EPA National Emission Inventory (NEI) (http://www.epa.gov/ttn/chief/net/2008inventory.html). Processing of these inventory data using SMOKE, provided chemical speciation and temporal and spatial allocation for area, point and mobile (both on-road and non-road) emission sources separately. For area and mobile sources, the province or county-total emissions were allocated to the WRF/Chem model grid cells through the use of gridding surrogates. We created 62 surrogate files for the US and 35 for Canada by processing a set of GIS shape files using the Surrogate Generator Tool, which can be found at http://www.ie.unc.edu/cempd/projects/mims/spatial/srgtool/SurrogateToolUserGuide.v3.6.htm. These surrogate files contain information on population, construction, agriculture, land use, etc., which can be modified for use in future scenario studies.

ACPD
13, 27937–27969, 2013

2.2.2 Biogenic emissions

Biogenic emissions were calculated online using the Model for Emissions of Gases and Aerosols from Nature (MEGAN) (Guenther et al., 2006). MEGAN is designed to give the net emission of gases and aerosols from terrestrial ecosystems into the atmosphere. It has been fully coupled into WRF/Chem to allow the online calculation of biogenic precursor emissions subject to the vegetation cover and existing meteorological conditions (temperature and solar radiation) at the time of the calculation (Grell et al., 2005).

3 Model evaluation

In order to establish the accuracy of the model's parameterizations and estimate the value of its scenario predictions, the WRF/Chem simulations were evaluated by comparison with available meteorological and chemical observations. Hourly meteorological measurements including T_2 (the temperature at 2 m above the surface), total precipitation and wind speed at 10 m were obtained from the National Climate Data and Information Archive (http://www.climate.weatheroffice.gc.ca) for Canada and from the Clean Air Status and Trends Network (CASNET; http://epa.gov/castnet/javaweb/index.html) for the US Hourly observations of surface $PM_{2.5}$ and Ozone concentrations were provided by the Canadian National Air Pollution Surveillance Network (NAPS; http://www.ec.gc.ca/natchem/default.asp?lang=en&n=EE0E2169-1) and by the United States Environmental Protection Agency (EPA; http://www.epa.gov/airdata).

Table 2 summarizes the month-by-month statistical evaluations for the meteorological variables and chemical species averaged over all stations for each month from April to August 2009. Comparisons of the model predictions and measured results for temperature and total daily precipitation are shown on maps of the model domain in Fig. 1a and b respectively. The measured results are shown inside the coloured circles, which also give the locations of the observation stations. Figure 1a shows that the spatial

ACPD
13, 27937–27969, 2013

distribution of T_2 is well reproduced by the model, despite a moderate over-prediction, especially for the spring months, that is evident in Table 2. The mean positive bias in T_2 ranges from +1.27 °C (40 %) in April to +0.57 °C (3.5 %) in July. These errors occur mostly in the high mid-latitudes, where the temperatures are most variable in the spring. They could be due to an inadequate description of the details of the large-scale polar circulation, which are not captured in our limited domain, or to a poor representation of the PBL, which is more variable during the spring. The model gives a much better description in the warmer months and in the southern part of the domain, where these meteorological conditions are more stable.

Figure 1b shows that the simulated total daily precipitation agrees quite well with observations everywhere in the domain except for a small over-prediction in parts of the southern-most states of the US, especially during the summer months. This is mostly due to difficulty in predicting intense convective rain, which is prevalent in this region. Table 2 shows that there is a systematic positive bias for daily precipitation, with the best performance in April (mean bias of +13.6 %) and worst in July (mean bias of +30.3 %). The model bias increases as the observed precipitation increases from April to July. Examination of the hourly time series for the individual months shows that most of the precipitation in the areas having the largest errors occurs during intense rain events associated with convective storms. Since these events are localized in space and time and there is only a small number (~10) of measurements in the part of the domain having the largest errors, the comparison also might be affected by the relatively coarse (12 km) spatial resolution of the model. While we are concerned by these biases, we note that they are comparable to or smaller than those reported previously in similar studies with WRF/Chem (Chuang et al., 2011; Zhang et al., 2010b) and also with CMAQ (Wu et al., 2008; Wang et al., 2009). Nevertheless, this result might indicate limitations in the WRF/Chem convective scheme, which could be a matter for future examination.

Hourly time series of the simulated and observed T_2, wind speed; O_3 and $PM_{2.5}$ are given in Fig. 2 from April to August 2009 at NAPS station #60 430. This station is

ACPD
13, 27937–27969, 2013

located in Toronto and is classified as urban, thus providing a severe test for the model. The model captures the T_2 diurnal cycle well at this location; the small (3.5 %) error in this case is largely due to under-prediction of the minimum nighttime temperatures.

The model reproduces the 10 m wind speed with a range of mean biases from +7.4 % in May to +21.4 % in August. The diurnal cycle of wind speed in Fig. 2 shows that the positive bias is largely due to under-prediction of low wind speeds at night. Better overall agreement is found in the spring months of April and May, when the observed wind speeds are slightly higher. This error also might be due to a poor description of the diurnal PBL height variation, but this performance is reasonable for a regional scale model. Similar or somewhat larger biases in wind speed predictions have been reported previously in comparable WRF/Chem studies (Zhang et al., 2010b; Chuang et al., 2011).

The monthly mean surface ozone is underestimated in the spring months, with mean biases of −25 % and −20 % in April and May, respectively and overestimated during the warmer months by 8.8 % (June), 22.4 % (July) and 14.4 % (August). Springtime underestimation and summertime overestimation of surface ozone also have been reported for similar WRF/Chem studies in both North America and Europe (Tuccella et al., 2012; Auvray and Bey, 2005; Zhang et al., 2010b; Yerramilli et al., 2010). Various factors are thought to contribute to these uncertainties, including the misrepresentation of background ozone through incorrect lateral boundary values and an inadequate description of photolysis radiation. We explored the effects of boundary conditions in two sets of simulations (not shown here), one of which used static default profiles and the other used time-dependent MOZART simulations. Not surprisingly, better performance (less underestimation) was found when MOZART data were used, so we used these for the results that we report here. While it is possible that the remaining errors might be due to incorrect MOZART boundary values, their seasonal dependence suggests the possibility of problems with the treatment of radiative transfer (or photochemistry) by WRF/Chem. It is beyond the scope of the present study to examine this in detail, but it might be a useful subject for future exploration.

ACPD
13, 27937–27969, 2013

The emission rates for this study were obtained from the inventories using the surrogate tools with SMOKE and the meteorology existing at the time of the calculation. This process is expected to produce results that are at least as accurate as those derived from interpolation of pre-processed inventories (Yerramilli et al., 2010; Zhang et al., 2010b); this is borne out by comparison of the biases shown in Table 2 with those reported by others using offline methods.

Table 2 shows that monthly mean $PM_{2.5}$ concentration is over-predicted in April, May and June by 21.4 %, 28.1 % and 31.2 % respectively, while the other two months have underestimations of −7.4 % and −21.2 % respectively. Most of the disagreement occurs during short, very large "spikes" of high particle concentrations that last only a few hours. Such events cannot be well described at the 12 km spatial scale of our model. Figure 2 shows, however, that the time dependence and long-term $PM_{2.5}$ averages are well reproduced by the model.

We conclude that the biases in the meteorological and chemical variables obtained in our WRF/Chem configuration are either smaller than or consistent with those obtained in other published studies. The uncertainties are sufficiently small to give us confidence that this configuration is suitable for future scenario studies designed to examine the effects of aerosols on precipitation.

4 Results and discussion

Figure 3 shows the spatial distribution of the five-month (April to August 2009) mean daily precipitation simulations. The total daily precipitation (left plot) is the sum of the convective (centre plot) and non-convective (right plot) precipitation. (Convective rain is the sub-gridscale rainfall parameterized by the convective cumulus scheme, while the non-convective part is the gridscale precipitation, calculated explicitly through the cloud microphysical processes in WRF/Chem.) This separation of rainfall in the model output provides a helpful tool to investigate thermal and microphysical (i.e. aerosol-induced) processes separately.

ACPD
13, 27937–27969, 2013

Figure 4 quantifies the seasonal contributions of convective and non-convective rain. It shows the monthly mean precipitation amounts from the different precipitation types integrated over all the monitoring sites indicated previously by circles in Fig. 1. It is evident that the cloud-resolved (non-convective) precipitation is more significant during April and May, while convective rain dominates in warmer periods due to greater tropospheric instability in the summer. The positive bias in the simulated total rain increases in warmer months as the convective precipitation increases – an observation that has been reported previously (Chen et al., 1998; Zhang et al., 2010b). The most probable cause of this seasonal dependence in the model bias for convective precipitation is the highly localized, rapidly varying nature of the latter, which makes the comparison of point measurements with predictions that are averaged over 12 km grid cells particularly difficult.

As shown in Figs. 1 and 3, the total daily precipitation averaged over five months has maxima over the central parts of the United States with highest amounts of about 9 mm day^{-1} in Kentucky and Tennessee. (Similarly heavy average rainfall of more than 10 mm day^{-1} also occurs off the Atlantic coast). Comparing the convective and non-convective plots in Fig. 3 shows that the heavy rainfall in the southern part of the domain is almost all convective and that the highest non-convective values (about 2–3 mm day^{-1}) occur further north, over central and south-eastern Canada.

A simple way to estimate the magnitude of the effects caused by the addition of chemistry to the simulation is to compare the results from WRF/Chem with those with the same WRF configuration, with the chemistry turned off. The lower panels in Fig. 3 show the differences obtained when the WRF (i.e. no chemistry) predictions of the five months mean precipitation are subtracted from those of WRF/Chem and broken down as total, convective and non-convective in the left, centre and right plots, respectively. The (WRF/Chem-WRF) difference plots for convective precipitation show that it is diminished in the southern part of the domain and increased in the northern part when chemistry is included. The effects of chemistry on non-convective rain have a higher degree of spatial variability, but it appears that the inclusion of chemistry causes a small,

ACPD
13, 27937–27969, 2013

but widespread increase in non-convective rain in the southern part of the domain and a pronounced increase near the heavily populated urban areas in the northeastern US coast.

The results shown in Fig. 3 can be interpreted in terms of models of aerosol-cloud interactions that have been developed over the past few years. The major influences of aerosols are direct radiative effects that affect convective rain by changing the thermal structure of the troposphere and indirect effects that modulate non-convective precipitation due to aerosol activation to CCN. As shown in the central panels of Fig. 3, there is a chemistry-induced decrease (around $-1\,\mathrm{mm\,day^{-1}}$ or approximately $-15\,\%$) in convective precipitation over the areas with high convective rain. This can be associated with additional surface cooling when chemistry is included, as is shown in the temperature difference plot in Fig. 5a. This surface cooling occurs predominantly in regions of high column-integrated $PM_{2.5}$ (see Fig. 5b), due to a combination of direct light scattering by the aerosols and by clouds nucleated by the aerosols. For the same reason, the warming effects over southeastern Canada shown in Fig. 5 are consistent with the increase in convective rain in the upper part of the domain that is seen in the difference plot in Fig. 3, an observation previously reported by (Zhang et al., 2010b) based on WRF/Chem simulations for July 2001. The two central panels of Fig. 3 also show that there is very little overall change in the very heavy convective rainfall over the Atlantic with the inclusion of chemistry – an observation that is also consistent with the fact that sea surface temperature is nearly invariant to inclusion of chemistry in the model (Fig. 5b).

The effects of chemistry on non-convective rain are also consistent with our understanding of the effects of aerosols on precipitation. Figure 3 shows that there is less non-convective rain in the southern part of the domain (top panel), but the chemistry-induced increase in non-convective rain (bottom panel) is larger there than in the north. Consistent with the above argument, we see a decrease in convective rain and an increase in non-convective rain in the eastern continental United States, which coincides with the locations of higher aerosol concentrations shown in Fig. 5b.

ACPD
13, 27937–27969, 2013

This pronounced chemistry-induced increase in non-convective precipitation (around +30 %) is evident in the difference plot of the heavily urbanized parts of the Atlantic coast (lower right panel, Fig. 3). To understand its origin, we took advantage of the explicit separation between activated (cloud-borne) aerosols and the remaining (interstitial) particles in the WRF/Chem output and plotted the spatial correlations of the various aerosol types with non-convective precipitation. The high-resolution plots in Fig. 6 show the result of this analysis. Figure 6a shows there is a strong increase in non-convective precipitation downwind of the heavily populated areas. (In this region, the predominant wind direction is east-north-east.) More detailed spatial correlations (not shown) indicated that small nitrate aerosols in the size range 0.1–1.0 µm had the highest spatial correlation with non-convective rain. Figure 6b shows the column integrated cloud-borne nitrate mass concentration. The correlation with increased non-convective rain is clear, a result that has also been reported previously (Ntelekos et al., 2009). Although we have not examined in detail the chemistry responsible for this, it seems reasonable to assume that the cloud-borne nitrates result from oxidation of NO_x by OH during the day and O_3 at night. In any case, we conclude from this that anthropogenic emissions from highly populated and industrialized locations have non-negligible influences on regional cloud formation and precipitation.

In order to elucidate further the possible microphysical influences of aerosols on precipitation, we analyzed the spatial correlation coefficients for the relevant variables. While correlations do not prove causality, they give good circumstantial evidence on which to base hypotheses (that will guide future experiments). The spatial correlation coefficients were calculated separately for activated (cloud-borne) particles and non-activated (interstitial) particles. Total aerosol mass concentrations were used for this part of the study; no chemical speciation was attempted. The results are shown in Figs. 7 and 8. The spatial correlation of column-integrated aerosols with cloud droplet number and non-convective precipitation is given in Fig. 7 for the size range 0.039–0.10 µm and in Fig. 8 for the 1.0–2.5 µm size range.

ACPD
13, 27937–27969, 2013

Not surprisingly, there is a strong positive correlation between cloud droplet number and cloud-borne aerosols of both sizes – i.e. the aerosols nucleate new cloud droplets or dissolve in existing cloud droplets or both. A positive, but weaker, correlation also exists between non-convective rain and cloud-borne aerosols of both sizes for similar reasons. There are strong differences, however, in the correlations involving interstitial aerosols of different sizes. Cloud droplet number and non-convective rain both correlate positively with small interstitial aerosols and negatively with larger interstitial particles. The high positive correlation between small interstitial aerosols and cloud droplet number is good evidence that the model correctly reproduces the first indirect aerosol effect – high cloud nucleation rates are caused by the (more numerous) small aerosols. The negative correlation between cloud droplet number and larger interstitial particles suggests that their removal by dissolution into existing cloud droplets is more rapid than their nucleation of new cloud droplets. The correlations involving non-convective rain: strongly positive for small particles and strongly negative for large particles are also consistent with this scenario. The former can be taken as evidence that the cloud droplets nucleated by the small particles eventually grow to produce non-convective precipitation. The latter simply indicates that larger interstitial aerosols are more efficiently removed by precipitation.

These general conclusions are framed in terms of the behaviour on large spatial scales, but the figures show interesting (and significant) deviations at local scales. One of these is the positive correlation between large interstitial aerosols and cloud droplet number that occurs downwind of Lakes Superior and Huron and the reduced anti-correlation with non-convective rain that occurs at the same location. While this is probably a purely physical effect involving the liquid aerosol droplets created by breaking waves at the eastern shore of this very large lake, it is an interesting demonstration of the ability of WRF/Chem to reproduce such micrometeorological phenomena.

ACPD
13, 27937–27969, 2013

5 Conclusions

Based on WRF/Chem v3.4 simulations with and without chemistry, we conclude that anthropogenic emissions and the atmospheric chemistry involving them have a significant effect on precipitation over north-eastern North America. The simulations covered the period from April to August 2009 in a domain with a 12 km horizontal grid resolution; they used temporally and spatially distributed emission fluxes from area, point and mobile sources produced using the SMOKE emission-processing model version 2.7. Evaluation of the results against available surface measurements for various meteorological variables and chemical compositions shows that the model reproduces these measurements very well. We also conclude that our configuration of the models for the domain of interest is suitable for scenario studies of the effects on precipitation of changes in total population and population distribution (as related to consequent changes in aerosols), because the biases we obtain are either smaller than or consistent with those obtained in other published studies using the same models.

The study shows that convective precipitation dominates in the summer and in the southern part of the domain due to greater tropospheric instability in warmer periods. Cloud-resolved (non-convective) rain is more significant during the spring, although the cloud-resolved precipitation contributes much less in total rain. A systematic overprediction is obvious in simulated monthly mean total daily rain. This positive bias increases in warmer months as the convective precipitation increases. This appears to be a common problem with the prediction convective precipitation, which is associated with its high spatial variability. This will have only a secondary effect on the planned scenario studies, however, because these will focus on anthropogenic effects on regional-scale precipitation.

WRF/Chem-WRF difference simulations show that the inclusion of chemistry decreases the convective rain in the southern (warmer) parts of domain and increases it in north. The reduction can be associated with increased stability due to surface cooling and upper-air warming when chemistry is included, but the spatial variations show

ACPD
13, 27937–27969, 2013

that the strength of these effects depends on local meteorology. The inclusion of chemistry results in a small increase in non-convective rain in southern parts of domain and a pronounced increase (around +30 %) near the heavily populated urban areas of the US Atlantic coast, which is consistent with the locations of higher $PM_{2.5}$ concentrations. A high-resolution view of the Atlantic coast shows a strong increase in non-convective rain downwind of heavily populated areas. Small nitrate aerosols in the size range 0.1–1.0 µm had the highest spatial correlation with non-convective rain in this region.

Spatial correlation coefficients for activated (cloud-borne) particles and non-activated (interstitial) particles in various size ranges elucidate some of the mechanisms causing these results. A strong positive correlation is found between cloud droplet number and cloud-borne aerosols in both small and large sizes indicating that aerosols nucleate new cloud droplets and dissolve in existing droplets. Also non-convective rain correlates positively with cloud-borne aerosols of all sizes for the same reason. Small and large non-activated (interstitial) aerosols, however, behave differently. Cloud droplet number and non-convective rain both correlate positively with small interstitial aerosols and both correlate negatively with larger interstitial particles. The positive correlation between small interstitial aerosols and cloud droplet number is consistent with the first indirect aerosol effect. The negative correlation between cloud droplet number and larger interstitial aerosols suggests that they are being removed by dissolution into existing cloud droplets more rapidly than they nucleate new cloud droplets. The strong positive (negative) correlations between small (large) interstitial aerosols and non-convective rain are also consistent with this scenario.

Acknowledgements. The authors are grateful to Ontario Power Generation (OPG) and the Natural Sciences and Engineering Research Council (NSERC) of Canada for financial support of this work. We are especially grateful to Rob Lyng for helpful comments and suggestions.

ACPD
13, 27937–27969, 2013

References

Abdul-Razzak, H. and Ghan, S. J.: A parameterization of aerosol activation – 3. Sectional representation, J. Geophys. Res.-Atmos., 107, 4026–4031, doi:10.1029/2001JD000483, 2002.

Ackerman, A. S., Toon, O. B., Stevens, D. E., Heymsfield, A. J., Ramanathan, V., and Welton, E. J.: Reduction of tropical cloudiness by soot, Science, 288, 1042–1047, doi:10.1126/science.288.5468.1042, 2000.

Albrecht, B. A.: Aerosols, cloud microphysics, and fractional cloudiness, Science, 245, 1227–1230, doi:10.1126/science.245.4923.1227, 1989.

Andreae, M. O., Rosenfeld, D., Artaxo, P., Costa, A. A., Frank, G. P., Longo, K. M., and Silva-Dias, M. A. F.: Smoking rain clouds over the Amazon, Science, 303, 1337–1342, doi:10.1126/science.1092779, 2004.

Auvray, M. and Bey, I.: Long-range transport to Europe: seasonal variations and implications for the European ozone budget, J. Geophys. Res.-Atmos., 110, D11303, doi:10.1029/2004JD005503, 2005.

Bell, T. L., Rosenfeld, D., Kim, K. M., Yoo, J. M., Lee, M. I., and Hahnenberger, M.: Midweek increase in US summer rain and storm heights suggests air pollution invigorates rainstorms, J. Geophys. Res.-Atmos., 113, D02209, doi:10.1029/2007JD008623, 2008.

Borys, R. D., Lowenthal, D. H., Cohn, S. A., and Brown, W. O. J.: Mountaintop and radar measurements of anthropogenic aerosol effects on snow growth and snowfall rate, Geophys. Res. Lett., 30, 1538, doi:10.1029/2002GL016855, 2003.

Chapman, E. G., Gustafson Jr., W. I., Easter, R. C., Barnard, J. C., Ghan, S. J., Pekour, M. S., and Fast, J. D.: Coupling aerosol-cloud-radiative processes in the WRF-Chem model: Investigating the radiative impact of elevated point sources, Atmos. Chem. Phys., 9, 945–964, doi:10.5194/acp-9-945-2009, 2009.

Chen, F. and Dudhia, J.: Coupling an advanced land surface-hydrology model with the Penn State-NCAR MM5 modeling system, Part I: Model implementation and sensitivity, Mon. Weather Rev., 129, 569–585, doi:10.1175/1520-0493(2001)129<0569:CAALSH>2.0.Co;2, 2001.

Chen, F., Mitchell, K., Janjic, Z., and Baldwin, M.: Impact of land-surface processes on the NCEP Eta model quantitative precipitation forecast, Special Symposium on Hydrology, 281–282, 1998.

ACPD
13, 27937–27969, 2013

Chou, M. D., Suarez, M. J., Ho, C. H., Yan, M. M. H., and Lee, K. T.: Parameterizations for cloud overlapping and shortwave single-scattering properties for use in general circulation and cloud ensemble models, J. Climate, 11, 202–214, doi:10.1175/1520-0442(1998)011<0202:Pfcoas>2.0.Co;2, 1998.

Chuang, M. T., Zhang, Y., and Kang, D. W.: Application of WRF/Chem-MADRID for real-time air quality forecasting over the southeastern United States, Atmos. Environ., 45, 6241–6250, doi:10.1016/j.atmosenv.2011.06.071, 2011.

Cotton, W. R. and Pielke Sr, R. A.: Human Impacts on Weather and Climate, Cambridge University Press, 2007.

Emmons, L. K., Walters, S., Hess, P. G., Lamarque, J.-F., Pfister, G. G., Fillmore, D., Granier, C., Guenther, A., Kinnison, D., Laepple, T., Orlando, J., Tie, X., Tyndall, G., Wiedinmyer, C., Baughcum, S. L., and Kloster, S.: Description and evaluation of the Model for Ozone and Related chemical Tracers, version 4 (MOZART-4), Geosci. Model Dev., 3, 43–67, doi:10.5194/gmd-3-43-2010, 2010.

Fast, J. D., Gustafson, W. I., Easter, R. C., Zaveri, R. A., Barnard, J. C., Chapman, E. G., Grell, G. A., and Peckham, S. E.: Evolution of ozone, particulates, and aerosol direct radiative forcing in the vicinity of Houston using a fully coupled meteorology-chemistry-aerosol model, J. Geophys. Res.-Atmos., 111, D21305, doi:10.1029/2005JD006721, 2006.

Givati, A. and Rosenfeld, D.: Quantifying precipitation suppression due to air pollution, J. Appl. Meteorol., 43, 1038–1056, doi:10.1175/1520-0450(2004)043<1038:Qpsdta>2.0.Co;2, 2004.

Grell, G. A. and Devenyi, D.: A generalized approach to parameterizing convection combining ensemble and data assimilation techniques, Geophys. Res. Lett., 29, 1693, doi:10.1029/2002GL015311, 2002.

Grell, G. A., Peckham, S. E., Schmitz, R., McKeen, S. A., Frost, G., Skamarock, W. C., and Eder, B.: Fully coupled "online" chemistry within the WRF model, Atmos. Environ., 39, 6957–6975, doi:10.1016/j.atmosenv.2005.04.027, 2005.

Guenther, A., Karl, T., Harley, P., Wiedinmyer, C., Palmer, P. I., and Geron, C.: Estimates of global terrestrial isoprene emissions using MEGAN (Model of Emissions of Gases and Aerosols from Nature), Atmos. Chem. Phys., 6, 3181–3210, doi:10.5194/acp-6-3181-2006, 2006.

ACPD
13, 27937–27969, 2013

Gustafson, W. I., Chapman, E. G., Ghan, S. J., Easter, R. C., and Fast, J. D.: Impact on modeled cloud characteristics due to simplified treatment of uniform cloud condensation nuclei during NEAQS 2004, Geophys. Res. Lett., 34, L19809, doi:10.1029/2007GL030021, 2007.

Haywood, J. and Boucher, O.: Estimates of the direct and indirect radiative forcing due to tropospheric aerosols: a review, Rev. Geophys., 38, 513–543, doi:10.1029/1999RG000078, 2000.

Haywood, J. M., Ramaswamy, V., and Soden, B. J.: Tropospheric aerosol climate forcing in clear-sky satellite observations over the oceans, Science, 283, 1299–1303, doi:10.1126/science.283.5406.1299, 1999.

Hong, S. Y., Noh, Y., and Dudhia, J.: A new vertical diffusion package with an explicit treatment of entrainment processes, Mon. Weather Rev., 134, 2318–2341, doi:10.1175/MWR3199.1, 2006.

Houyoux, M. R. and Vukovich, J. M.: Updates to the Sparse Matrix Operator Kernel Emissions (SMOKE) Modeling System and Integration with Models-3, The Emission Inventory: Regional Strategies for the Future, Air & Waste Management Association Raleigh, NC, 1999.

IPCC: Climate changes 2007: the physical sciences basis, in: Contribution of Working Group I to the Fourth Assemssment Report of the Intergovernmental Panel on Climate Change, edited by: Solomon, S., Qin, D., and Manning, M., 2007.

Khain, A., Arkhipov, V., Pinsky, M., Feldman, Y., and Ryabov, Y.: Rain enhancement and fog elimination by seeding with charged droplets, Part I: Theory and numerical simulations, J. Appl. Meteorol., 43, 1513–1529, doi:10.1175/JAM2131.1, 2004.

Khain, A., Rosenfeld, D., and Pokrovsky, A.: Aerosol impact on the dynamics and microphysics of deep convective clouds, Q. J. Roy. Meteor. Soc., 131, 2639–2663, doi:10.1256/QJ.04.62, 2005.

Koren, I., Kaufman, Y. J., Rosenfeld, D., Remer, L. A., and Rudich, Y.: Aerosol invigoration and restructuring of Atlantic convective clouds, Geophys. Res. Lett., 32, L14828, doi:10.1029/2005GL023187, 2005.

Lin, Y. L., Farley, R. D., and Orville, H. D.: Bulk parameterization of the snow field in a cloud model, J. Climate Appl. Meteorol., 22, 1065–1092, doi:10.1175/1520-0450(1983)022<1065:Bpotsf>2.0.Co;2, 1983.

Lohmann, U. and Feichter, J.: Global indirect aerosol effects: a review, Atmos. Chem. Phys., 5, 715–737, doi:10.5194/acp-5-715-2005, 2005.

Lohmann, U. and Hoose, C.: Sensitivity studies of different aerosol indirect effects in mixed-phase clouds, Atmos. Chem. Phys., 9, 8917–8934, doi:10.5194/acp-9-8917-2009, 2009.

ACPD
13, 27937–27969, 2013

Lynn, B., Khain, A., Rosenfeld, D., and Woodley, W. L.: Effects of aerosols on precipitation from orographic clouds, J. Geophys. Res.-Atmos., 112, D10225, doi:10.1029/2006JD007537, 2007.

McKeen, S., Chung, S. H., Wilczak, J., Grell, G., Djalalova, I., Peckham, S., Gong, W., Bouchet, V., Moffet, R., Tang, Y., Carmichael, G. R., Mathur, R., and Yu, S.: Evaluation of several $PM_{2.5}$ forecast models using data collected during the ICARTT/NEAQS 2004 field study, J. Geophys. Res.-Atmos., 112, D10S20, doi:10.1029/2006JD007608, 2007.

Mlawer, E. J., Taubman, S. J., Brown, P. D., Iacono, M. J., and Clough, S. A.: Radiative transfer for inhomogeneous atmospheres: RRTM, a validated correlated-k model for the longwave, J. Geophys. Res.-Atmos., 102, 16663–16682, doi:10.1029/97JD00237, 1997.

Ntelekos, A. A., Smith, J. A., Donner, L., Fast, J. D., Gustafson, W. I., Chapman, E. G., and Krajewski, W. F.: The effects of aerosols on intense convective precipitation in the north-eastern United States, Q. J. Roy. Meteor. Soc., 135, 1367–1391, doi:10.1002/QJ.476, 2009.

Penner, J. E., Dong, X. Q., and Chen, Y.: Observational evidence of a change in radiative forcing due to the indirect aerosol effect, Nature, 427, 231–234, doi:10.1038/Nature02234, 2004.

Ramanathan, V., Crutzen, P. J., Kiehl, J. T., and Rosenfeld, D.: Atmosphere – aerosols, climate, and the hydrological cycle, Science, 294, 2119–2124, doi:10.1126/science.1064034, 2001.

Rosenfeld, D.: Suppression of rain and snow by urban and industrial air pollution, Science, 287, 1793–1796, doi:10.1126/science.287.5459.1793, 2000.

Rosenfeld, D. and Givati, A.: Evidence of orographic precipitation suppression by air pollution-induced aerosols in the western United States, J. Appl. Meteorol. Clim., 45, 893–911, doi:10.1175/JAM2380.1, 2006.

Rosenfeld, D., Lahav, R., Khain, A., and Pinsky, M.: The role of sea spray in cleansing air pollution over ocean via cloud processes, Science, 297, 1667–1670, doi:10.1126/science.1073869, 2002.

Rosenfeld, D., Kaufman, Y. J., and Koren, I.: Switching cloud cover and dynamical regimes from open to closed Benard cells in response to the suppression of precipitation by aerosols, Atmos. Chem. Phys., 6, 2503–2511, doi:10.5194/acp-6-2503-2006, 2006.

Rosenfeld, D., Khain, A., Lynn, B., and Woodley, W. L.: Simulation of hurricane response to suppression of warm rain by sub-micron aerosols, Atmos. Chem. Phys., 7, 3411–3424, doi:10.5194/acp-7-3411-2007, 2007.

ACPD
13, 27937–27969, 2013

Rosenfeld, D., Lohmann, U., Raga, G. B., O'Dowd, C. D., Kulmala, M., Fuzzi, S., Reissell, A., and Andreae, M. O.: Flood or drought: how do aerosols affect precipitation?, Science, 321, 1309–1313, doi:10.1126/science.1160606, 2008.

Rudich, Y., Khersonsky, O., and Rosenfeld, D.: Treating clouds with a grain of salt, Geophys. Res. Lett., 29, 2060, doi:10.1029/2002GL016055, 2002.

Tao, W. K., Li, X. W., Khain, A., Matsui, T., Lang, S., and Simpson, J.: Role of atmospheric aerosol concentration on deep convective precipitation: cloud-resolving model simulations, J. Geophys. Res.-Atmos., 112, D24S18, doi:10.1029/2007JD008728, 2007.

Taubman, B. F., Marufu, L. T., Vant-Hull, B. L., Piety, C. A., Doddridge, B. G., Dickerson, R. R., and Li, Z. Q.: Smoke over haze: aircraft observations of chemical and optical properties and the effects on heating rates and stability, J. Geophys. Res.-Atmos., 109, D02206, doi:10.1029/2003JD003898, 2004.

Tuccella, P., Curci, G., Visconti, G., Bessagnet, B., Menut, L., and Park, R. J.: Modeling of gas and aerosol with WRF/Chem over Europe: evaluation and sensitivity study, J. Geophys. Res.-Atmos., 117, D03303, doi:10.1029/2011JD016302, 2012.

Twomey, S. A.: Pollution and cloud albedo, Eos T. Am. Geophys. Un., 58, 797–797, 1977.

Wang, K., Zhang, Y., Jang, C., Phillips, S., and Wang, B. Y.: Modeling intercontinental air pollution transport over the trans-Pacific region in 2001 using the Community Multiscale Air Quality modeling system, J. Geophys. Res.-Atmos., 114, D04307, doi:10.1029/2008JD010807, 2009.

Wild, O., Zhu, X., and Prather, M. J.: Fast-j: Accurate simulation of in- and below-cloud photolysis in tropospheric chemical models, J. Atmos. Chem., 37, 245–282, doi:10.1023/A:1006415919030, 2000.

Williams, E., Rosenfeld, D., Madden, N., Gerlach, J., Gears, N., Atkinson, L., Dunnemann, N., Frostrom, G., Antonio, M., Biazon, B., Camargo, R., Franca, H., Gomes, A., Lima, M., Machado, R., Manhaes, S., Nachtigall, L., Piva, H., Quintiliano, W., Machado, L., Artaxo, P., Roberts, G., Renno, N., Blakeslee, R., Bailey, J., Boccippio, D., Betts, A., Wolff, D., Roy, B., Halverson, J., Rickenbach, T., Fuentes, J., and Avelino, E.: Contrasting convective regimes over the Amazon: implications for cloud electrification, J. Geophys. Res.-Atmos., 107, 8082, doi:10.1029/2001jd000380, 2002.

Wu, S. Y., Krishnan, S., Zhang, Y., and Aneja, V.: Modeling atmospheric transport and fate of ammonia in North Carolina – Part I: Evaluation of meteorological and chemical predictions, Atmos. Environ., 42, 3419–3436, doi:10.1016/j.atmosenv.2007.04.031, 2008.

ACPD
13, 27937–27969, 2013

Xue, Y., Zeng, F. J., Mitchell, K. E., Janjic, Z., and Rogers, E.: The impact of land surface processes on simulations of the US hydrological cycle: a case study of the 1993 flood using the SSiB land surface model in the NCEP Eta regional model, Mon. Weather Rev., 129, 2833–2860, doi:10.1175/1520-0493(2001)129<2833:Tiolsp>2.0.Co;2, 2001.

Yerramilli, A., Challa, V. S., Dodla, V. B. R., Dasari, H. P., Young, J. H., Patrick, C., Baham, J. M., Hughes, R. L., Hardy, M. G., and Swanier, S. J.: Simulation of surface ozone pollution in the central Gulf coast region using WRF/Chem model: sensitivity to PBL and land surface physics, Adv. Meteorol., 2010, 319138, doi:10.1155/2010/319138, 2010.

Zaveri, R. A. and Peters, L. K.: A new lumped structure photochemical mechanism for large-scale applications, J. Geophys. Res.-Atmos., 104, 30387–30415, doi:10.1029/1999JD900876, 1999.

Zaveri, R. A., Easter, R. C., Fast, J. D., and Peters, L. K.: Model for Simulating Aerosol Interactions and Chemistry (MOSAIC), J. Geophys. Res., 113, D13204, doi:10.1029/2007JD008782, 2008.

Zhang, Y., Pan, Y., Wang, K., Fast, J. D., and Grell, G. A.: WRF/Chem-MADRID: incorporation of an aerosol module into WRF/Chem and its initial application to the TexAQS2000 episode, J. Geophys. Res.-Atmos., 115, D18202, doi:10.1029/2009JD013443, 2010a.

Zhang, Y., Wen, X. Y., and Jang, C. J.: Simulating chemistry-aerosol-cloud-radiation-climate feedbacks over the continental US using the online-coupled Weather Research Forecasting Model with chemistry (WRF/Chem), Atmos. Environ., 44, 3568–3582, doi:10.1016/j.atmosenv.2010.05.056, 2010b.

ACPD
13, 27937–27969, 2013

Table 1. The WRF/Chem configuration options used in this study.

Atmospheric processes	Model option	Reference
Meteorology		
Longwave radiation	RRTM	Mlawer et al. (1997)
Shortwave radiation	Goddard	Chou et al. (1998)
Land surface model	Noah LSM	Chen and Dudhia (2001)
Boundary layer	YSU	Hong et al. (2006)
Cumulus	Grell 3-D	Grell and Devenyi (2002)
Cloud microphysics	Lin et al.	Lin et al. (1983)
Chemistry		
Photolysis	Fast-J	Wild et al. (2000)
Gas-phase chemistry	CBM-Z	Zaveri and Peters (1999)
Aerosol scheme	MOSAIC	Zaveri et al. 2008)
Chemical boundary conditions	MOZART 4	Emmons et al. (2010)
Anthropogenic emissions	Processed by SMOKE 2.7	Houyoux and Vukovich (1999)
Biogenic emissions	MEGAN	Guenther et al. (2006)

ACPD
13, 27937–27969, 2013

Table 2. Summary of the evaluation of WRF/Chem simulations from Apr to Aug 2009 by comparison with ground-based meteorological and chemical measurements.

	Variables	Month	Stations	Mean Obs	Mean Model	RMSE	Bias	
							Mean	%
Meteorology	Total Daily rain ($mm\,day^{-1}$)	Apr	105	2.50	2.84	4.56	0.34	13.6
		May	105	2.25	2.66	4.57	0.37	16.4
		Jun	105	2.74	3.52	7.03	0.84	30.7
		Jul	105	3.39	4.42	8.01	1.03	30.4
		Aug	105	3.38	4.12	8.29	0.72	21.3
	T_2 (°C)	Apr	95	3.15	4.51	3.24	1.27	40.3
		May	95	8.49	10.26	3.81	1.77	20.8
		Jun	95	14.32	15.06	3.41	0.83	5.8
		Jul	95	16.12	16.68	3.20	0.57	3.5
		Aug	95	16.77	17.75	3.04	0.99	5.9
	Wind Speed at 10 m ($m\,s^{-1}$)	Apr	95	4.38	4.81	2.23	0.42	9.6
		May	95	4.18	4.48	2.37	0.31	7.4
		Jun	95	3.56	3.98	2.07	0.43	12.1
		Jul	95	3.41	4.04	2.11	0.64	18.8
		Aug	95	3.40	4.14	2.14	0.73	21.5
Chemistry	Ozone (ppb)	Apr	109	36.66	27.46	13.54	−9.19	−25.1
		May	109	32.00	25.49	15.57	−6.55	−20.5
		Jun	109	26.01	28.29	11.29	2.28	8.8
		Jul	109	21.08	25.78	10.79	4.73	22.4
		Aug	109	23.36	25.73	12.96	3.37	14.4
	$PM_{2.5}$ ($\mu g\,m^{-3}$)	Apr	64	5.08	6.14	6.04	1.09	21.5
		May	64	5.84	7.48	7.86	1.64	28.1
		Jun	64	6.02	7.87	8.67	1.88	31.2
		Jul	64	6.73	6.23	5.63	−0.50	−7.4
		Aug	64	9.39	7.42	8.10	−1.99	−21.2

ACPD
13, 27937–27969, 2013

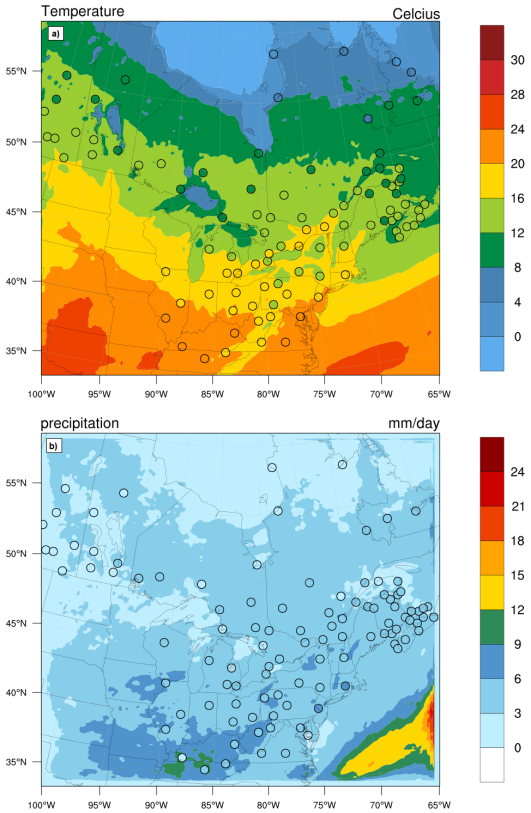

Fig. 1. Observed and simulated 2 m Temperature **(a)** and total daily precipitation **(b)** averaged for five months (April–August 2009). Measurements are shown as circles with the same colour scale as the simulations.

ACPD
13, 27937–27969, 2013

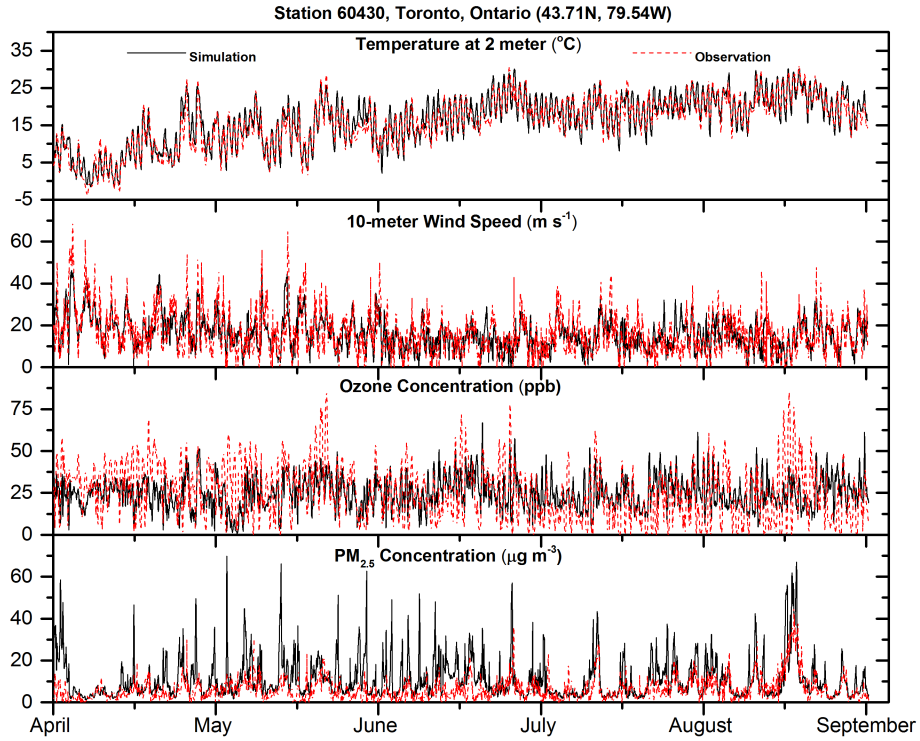

Fig. 2. Simulated and observed time series of hourly Temperature at 2 m above the surface, wind speed at 10 m, surface Ozone and $PM_{2.5}$ concentrations from April to August 2009 at station 60 430 located in Toronto.

ACPD
13, 27937–27969, 2013

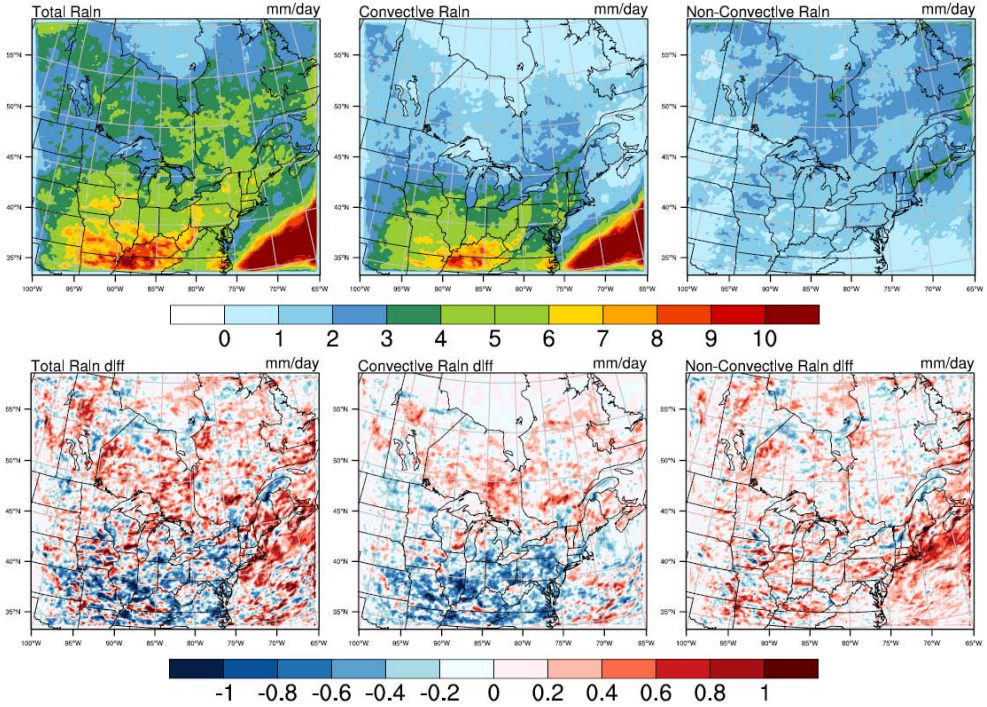

Fig. 3. Spatial distribution of five month mean (April–August 2009) simulated total daily precipitation (left), convective (centre) and non-convective rain (right) by WRF/Chem (top) and the difference (WRF/Chem – WRF) (bottom).

ACPD
13, 27937–27969, 2013

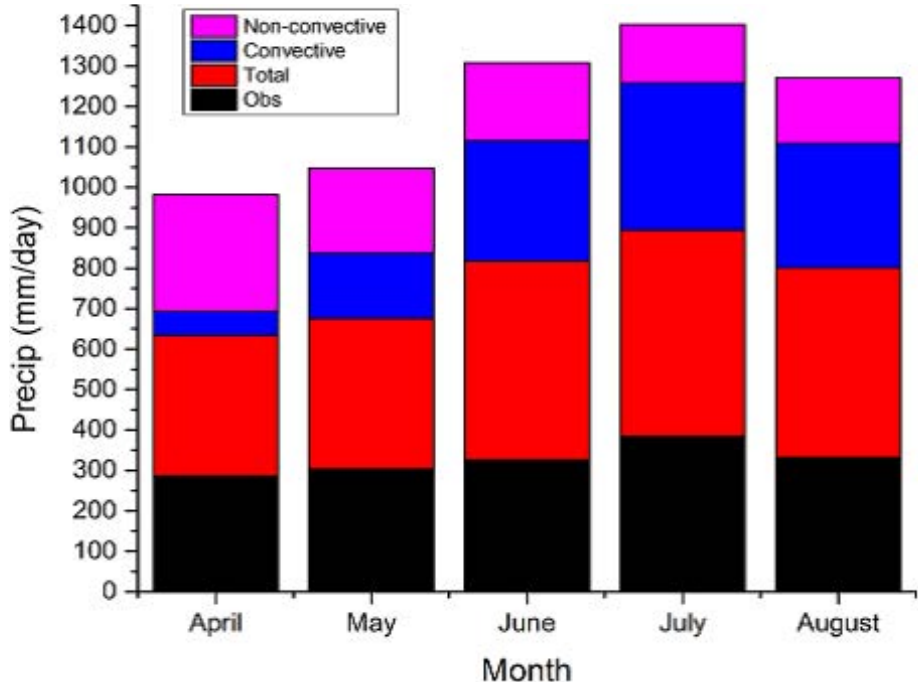

Fig. 4. Total observed and simulated daily precipitation integrated over all the monitoring sites shown in Fig. 1.

ACPD
13, 27937–27969, 2013

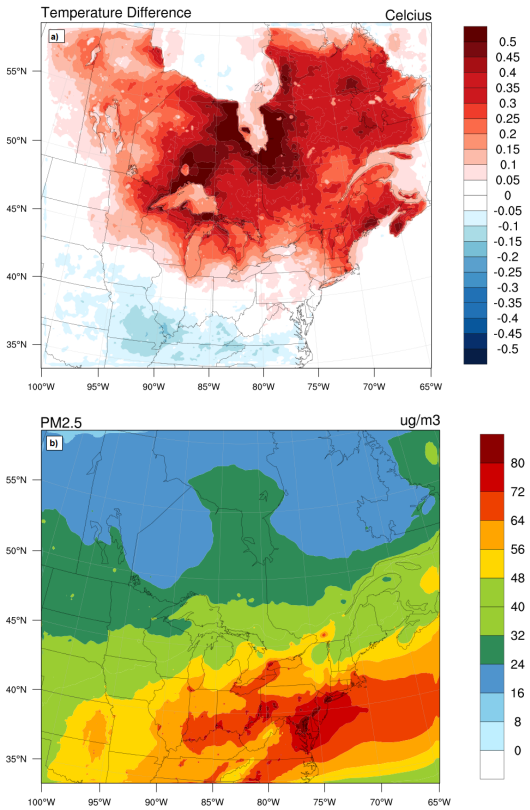

Fig. 5. Simulated spatial distributions of: **(a)** five month mean (April to August 2009) WRF/Chem-WRF Temperature at 2 m; **(b)** WRF/Chem column-integrated mass concentration of $PM_{2.5}$.

ACPD
13, 27937–27969, 2013

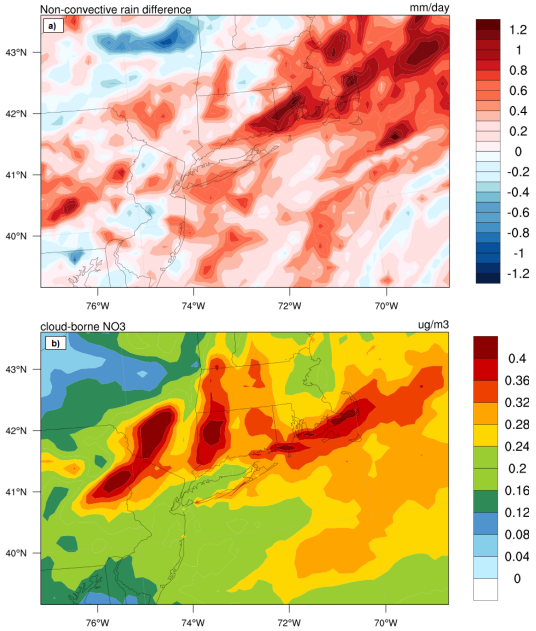

Fig. 6. Spatial distributions of five month mean (April to August 2009) non-convective WRF/Chem-WRF rain difference (top) and the column integrated cloud-borne Nitrate (bottom).

ACPD
13, 27937–27969, 2013

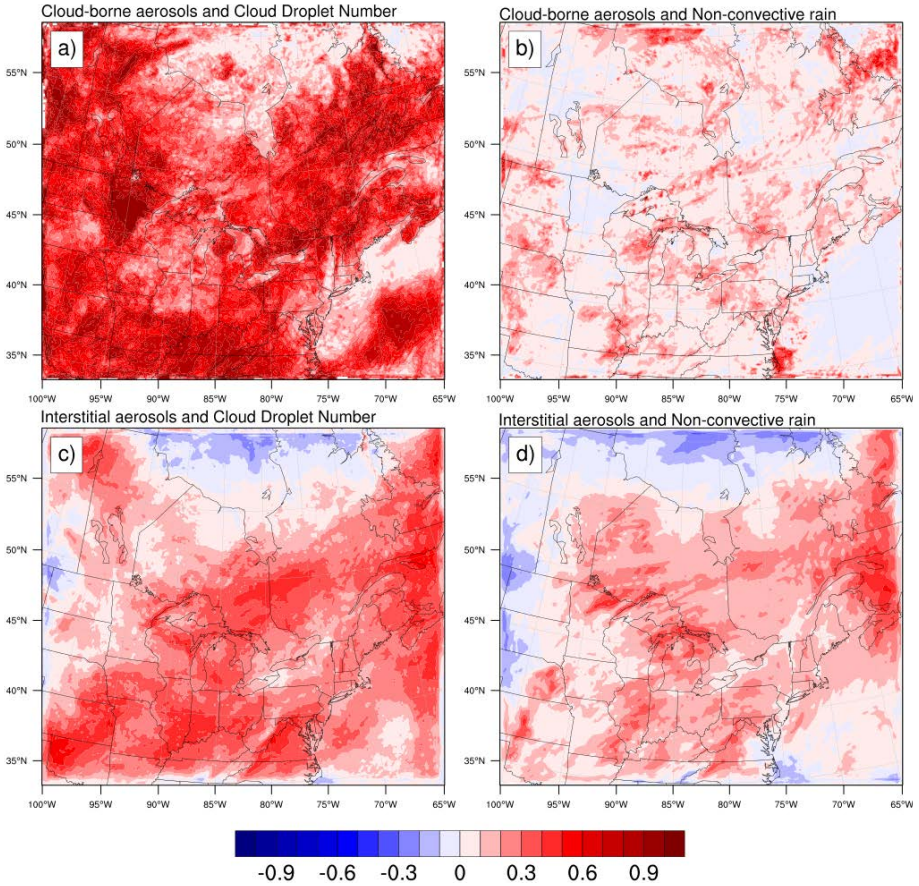

Fig. 7. Correlation between simulated WRF/Chem cloud droplet number (left) and non-convective rain (right), with column-integrated cloud-borne (top) and interstitial (bottom) for size range 0.039–0.1 µm.

ACPD
13, 27937–27969, 2013

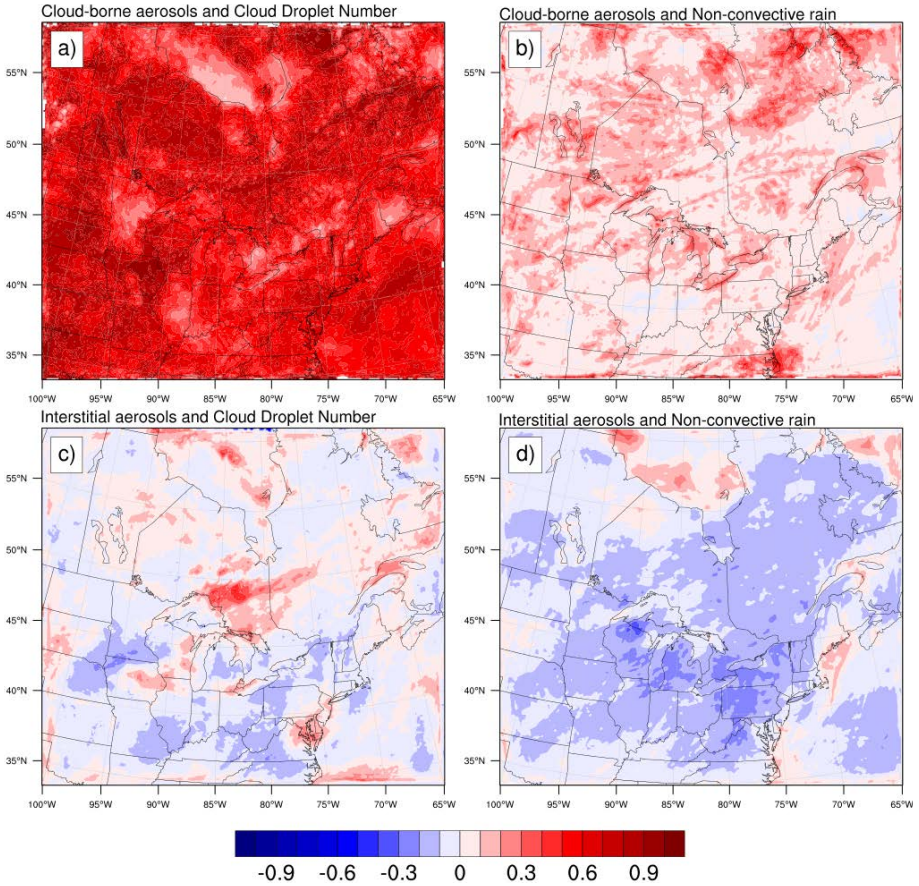

Fig. 8. Correlation between simulated WRF/Chem cloud droplet number (left) and non-convective rain (right), with column-integrated cloud-borne (top) and interstitial (bottom) for size range 1–2.5 µm.

ACPD
13, 27937–27969, 2013